

## Adsorption dynamics and equilibrium studies of Zn (II) onto chitosan

G KARTHIKEYAN\*, K ANBALAGAN and N MUTHULAKSHMI ANDAL

Department of Chemistry, Gandhigram Rural Institute – Deemed University, Gandhigram 624 302, India  
e-mail: drg\_karthikeyan@rediffmail.com

MS received 3 June 2003; revised 12 November 2003

**Abstract.** Batch equilibration studies are conducted to determine the nature of adsorption of zinc (II) over chitosan. The factors affecting the adsorption process like particle size, contact time, dosage, pH, effects of chloride and nitrate are identified. The influence of temperature and co-ions on the adsorption process is verified. The fraction of adsorption,  $Y_t$  and the intraparticle diffusion rate constant,  $k_p$  are calculated at different environments and the results are discussed. The nature of adsorption of the zinc (II)–chitosan system is explained using Freundlich, Langmuir isotherms and thermodynamic parameters.

**Keywords.** Adsorption dynamics; chitosan; pH; fraction of adsorption; intraparticle diffusion; co-ions.

### 1. Introduction

Zinc occurring in the earth's crust at an average concentration of 70 mg/kg is classified as a borderline metal. Under aerobic conditions,  $Zn^{2+}$  is the predominant species at acidic pH, but it is replaced by  $Zn(OH)_2$  at pH 8–11.<sup>1</sup> Ingestion of >2 g zinc produces toxic symptoms (fever, diarrhoea and gastrointestinal tract irritation) in humans. There are also many incidents of extensive mortality and/or contamination of fish and other aquatic species from the discharge of zinc-containing wastewater.

The present study deals with the sorption of zinc (II) by chitosan, a deacetylated product of chitin as an adsorbent. Chitosan is obtained by deacetylation of chitin, which is extracted from the shells of shrimps, crabs and other crustaceans and some fungi.<sup>2</sup> Chitosan chelates five to six times greater amounts of metals than chitin.<sup>3</sup> This is attributed to the deacetylation process. Chitosan has many useful features e.g. hydrophilicity, biocompatibility, biodegradability, anti-bacterial property and remarkable affinity for many proteins.<sup>4</sup> This polymer is a well known sorbent, effective in the uptake of metal ions, since the amine groups on the chitosan chain can serve as chelation sites for metals. The mechanism by which metal ions are bound by chitosan probably involves attachment of these ions to  $-NH_2$  groups. Because of this difference, it may be suit-

able for scavenging important heavy metal ions and complexes that cannot be adequately treated by other natural polymers.<sup>5,6</sup> Guibal *et al*<sup>7</sup> studied the enhancement of metal ion sorption performances of chitosan. Chitosan displayed a surface controlled sorption mechanism, indicating a monolayer sorption with interactions between the sorbed molecules and heterogeneous distribution of sorption energies. Chitosan interaction with metal ions has also been studied by Schmuhl *et al*<sup>8</sup>.

### 2. Experimental

The raw sample of chitosan was supplied by M/s BR Corporation, Mumbai, in the form of coarse grains. Chitosan was pulverized and sieved into two grades, 0.21 mm and 0.71 mm. The materials with different dimensions were treated with 0.1 N hydrochloric acid and 0.1 N sodium hydroxide for three hours each. The purified samples were washed several times with double distilled water till it registered neutral pH, as swelling would make more sites available. Later the samples were dried in an oven. All the chemicals employed for the analysis were either AnalaR, GR or other high purity grade and used without further purification. Zinc sulphate, sodium chloride, sodium nitrate, hydrochloric acid and sodium hydroxide were used for the experiments. The experiments were performed using double distilled water.

\*For correspondence

From the stock solution containing 1000 mg/L of zinc ions, aliquots of the adsorbate containing varying concentrations from 2–14 mg/L of zinc ions were prepared. 50 ml of the same was mixed with 10 mg each of two grades of chitosan and the mixtures were agitated in a mechanical shaker. The solution was filtered at preset time intervals (2 min) and the residual metal ion concentrations were measured using Atomic Absorption Spectrometer (Model AA 100, Perkin Elmer make). The experiments were conducted at four different temperatures, viz., 293 K, 303 K, 313 K and 323 K using a thermostat attached with a shaker, TECHNO make whose accuracy is within  $\pm 0.5^\circ\text{C}$ . Adsorption studies of zinc (II) ions in the presence of three metal ions viz., iron (III), copper (II) and chromium (VI) were experimentally verified to study the effect of co-ions. This involved the determination of the residual zinc (II) ions in the mixture containing equal amounts of iron (III), copper (II) and chromium (VI) ions. The pH was measured using Elico L1 120 pH meter. Duplicate measurements were also conducted to ensure the reproducibility of the values of residual concentration within  $\pm 2\%$ .

### 3. Results and discussion

#### 3.1 Effect of particle size

The adsorption rate of zinc ions by chitosan with two particle sizes (0.21 and 0.50 mm) is illustrated in figure 1 and the values are given in table 1. It is

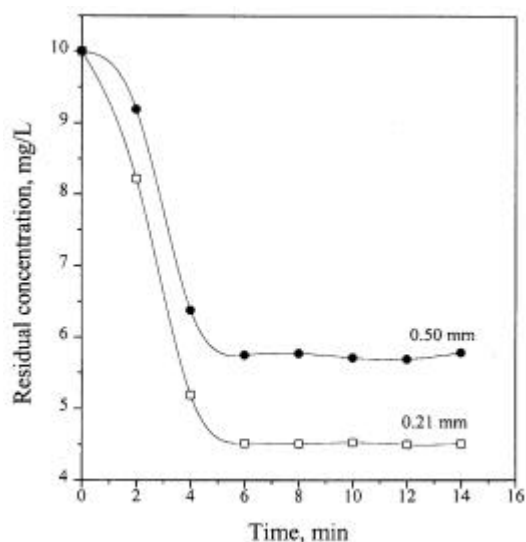


**Figure 1.** Effect of particle size.

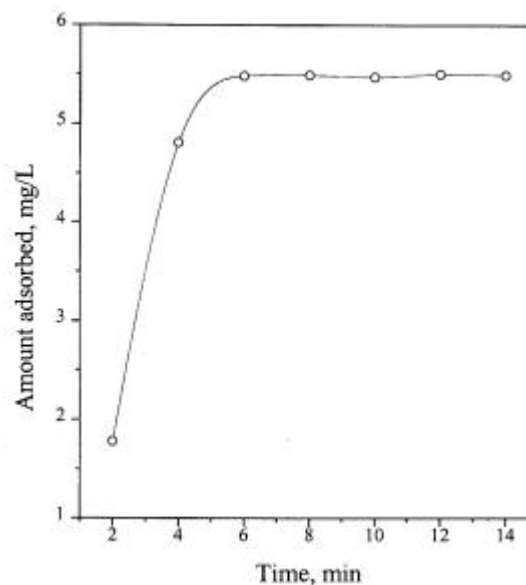


**Figure 2.** Effect of contact time.

**Table 1.** Effect of particle size.

Time (min)	Concentration (mg/L)	
	0.21 mm	0.50 mm
0	10.00	10.00
2	8.22	9.79
4	5.19	6.38
6	4.52	5.75
8	4.51	5.77
10	4.53	5.71
12	4.50	5.69
14	4.51	5.78

Initial concentration of zinc ions  $[\text{Zn}]_0 = 10 \text{ mg/L}$ ;  
pH = 7; temperature = 303 K; adsorbant dose = 10 mg

**Table 2.** Effect of contact time.

Time (min)	Amount adsorbed (mg/L)
2	1.78
4	4.81
6	5.48
8	5.49
10	5.47
12	5.50
14	5.49

Initial concentration of zinc ions  $[\text{Zn}]_0 = 10 \text{ mg/L}$ ;  
pH = 7; temperature = 303 K; adsorbant dose = 10 mg

evident from the table that the concentration of zinc (II) adsorbed decreases with an increase in the particle size of chitosan, explaining the diminishing sorption rate at large dimensions. High rate of adsorption by chitosan with smaller particle sizes is due to the availability of more specific surface area on the adsorbent. According to Weber and Morris,<sup>9</sup> the breaking of larger particles tends to open tiny cracks and channels on the particle surface of the material resulting in more accessibility to better diffusion, owing to the smaller particle size.<sup>10</sup>

### 3.2 Effect of contact time

The nature of the adsorption of zinc (II) on chitosan is illustrated in figure 2 and the experimental results are given in table 2. An initial steep increase in the adsorption curve followed by a bend at the sixth minute was observed. No further adsorption of zinc (II) was evident and this indicated the formation of an equilibrium at the sixth minute.

### 3.3 Effect of dose

The experimental results using three doses viz. 10, 20 and 30 mg of chitosan and 10 mg/L of zinc (II) revealed a definite increase in the adsorption capacity of chitosan with dosage. This is due to the larger number of available adsorption sites favouring the enhanced uptake of the metal ion. The dependence of adsorption on doses can be explained in terms of the concentration factor involving low metal-to-adsorbent ratio at low metal concentrations. Subsequently, fractional adsorption becomes independent of initial concentration. However, at higher concentrations, the available sites of adsorption become fewer and hence the percentage of metal ion removed is dependent upon the initial concentration.<sup>11</sup> The rate of adsorption was appreciable at an initial dose of 10 mg of chitosan although at its higher doses the rate registered an increase. However, a proportionate increase in the rate was absent at higher doses. In view of this, 10 mg of chitosan was fixed as the dose for the remaining experiments along with 0.21 mm particle size and six minutes contact time as the optimum conditions for the further experiments.

### 3.4 Effect of pH

The sorption characteristics of chitosan determined at pH 3, 5, 7 and 8 against time is illustrated in figure 3.

The system is strongly pH dependent, because the properties of both the chitosan surface (charge and potential) and the solution composition (metal ion speciation) change with pH.<sup>12</sup> The number of active sites on the surface of the adsorbent may change with varying pH. The rate of adsorption is maximum at pH 7. Table 3 explains the details of the residual concentrations of zinc (II) in solution at definite time intervals at four pH levels. The sorption rate is lower at acidic and alkaline ranges. Low pH would favour protonation of the amino sites on the surface, resulting in a reversal of charge leading to a reduction in the chelating ability of chitosan.<sup>8</sup> At alkaline range, the formation of Zn(OH)<sub>2</sub> complexes prevent further adsorption of zinc (II).

### 3.5 Effect of chloride and nitrate

The adsorption of zinc (II) by chitosan in presence of excess chloride is shown in figure 4. The percent-

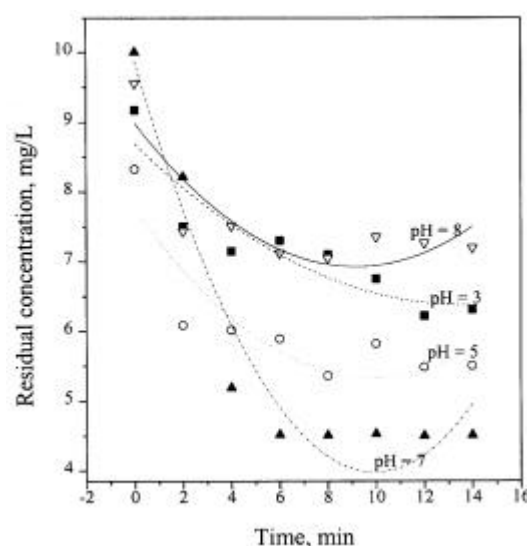
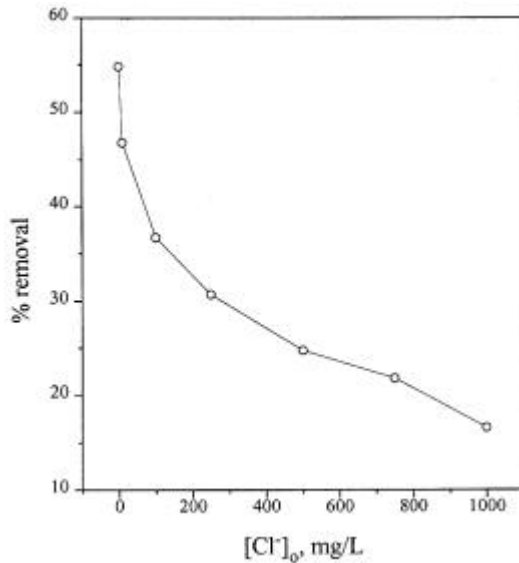


Figure 3. Effect of pH.

Table 3. Effect of pH.

Time (min)	Concentration (mg/L)			
	pH = 3	pH = 5	pH = 7	pH = 8
0	9.17	8.33	10.00	9.55
2	7.50	6.09	8.22	7.43
4	7.15	6.02	5.19	7.51
6	7.30	5.89	4.52	7.12
8	7.10	5.36	4.51	7.05
10	6.75	5.82	4.53	7.35
12	6.22	5.48	4.50	7.26
14	6.31	5.50	4.51	7.28

Initial concentration of zinc ions  $[Zn]_0 = 10$  mg/L; temperature = 303 K; adsorbant dose = 10 mg



**Figure 4.** Effect of chloride ion concentration.

**Table 4.** Time dependence of the fraction of adsorption at different particle sizes.

$T^{1/2}$ (min <sup>1/2</sup> )	$Y_t$	
	0.21 mm	0.50 mm
0	0	0
1.41	0.32	0.19
2.00	0.87	0.85
2.45	1.00	1.00
2.83	0.95	1.00
3.16	0.94	1.01
3.46	0.95	1.01
3.76	0.94	0.99

**Table 5.** Time dependence of the fraction of adsorption at different amounts.

$t^{1/2}$ (min <sup>1/2</sup> )	$Y_t$		
	10 mg	20 mg	30 mg
0	0	0	0
1.41	0.32	0.63	0.89
2.00	0.87	0.94	0.94
2.45	1.00	1.00	1.00
2.83	0.95	1.04	1.01
3.16	0.94	1.03	1.01
3.46	0.95	0.99	1.00
3.76	0.94	1.03	1.00

age of zinc (II) removed by chitosan decreased at higher concentrations of chloride ions. The inhibi-

tion in the sorption rate of chitosan is due to the affinity between  $Zn^{2+}$  ions and  $Cl^-$  ions. The low adsorption rate of zinc ions viz., 16.6% at a concentration of 1000 mg/L of  $Cl^-$  in the solution is due to the formation of zinc chloride. That is, the amount of free zinc ions remaining in solution for adsorption is reduced considerably and hence the low adsorption rate of zinc ions. Our findings are in good agreement with the observations of earlier workers.<sup>13,14</sup> A similar inhibitory trend in the adsorption of zinc was observed in nitrate environment also. A gradual reduction in the adsorption rate resulted at higher concentrations of nitrate ions. The adsorption rate of zinc (II) is reduced to half of its original value, as observed at 500 mg/L of  $NO_3^-$  amounting to a reduction from 54.80% to 26.35%.

### 3.6 Time dependence of the fraction of adsorption at different particle sizes and doses of chitosan

Time dependence (tables 4 and 5) is determined by plotting the fraction of adsorption,  $Y_t = C_0 - C_t/C_0 - C_e$  against the retention time,  $t^{1/2}$ , where  $C_0$  denotes the initial concentration of metal ions,  $C_t$ , the concentration of metal ions at the preset time intervals and  $C_e$ , the equilibrium concentration. The rate of fraction of adsorption,  $Y_t$ , expressed as square root of time,<sup>7</sup> is estimated from the three-staged curves illustrated for different particle sizes and doses of chitosan as shown in figures 5 and 6. The initial stage of the curves relate to the transfer of metal ions from the bulk of solution to the boundary film of the adsorbent and later to its surface. The second stage, corresponds to the transfer of the metal ions from the surface to the intraparticle active sites of chitosan. This stage is the rate-determining step of the reaction. The final stage shows the completion of sorption reaching an equilibrium.<sup>15</sup> At equilibrium, there is a defined distribution of the solute particle between the solution and the solid chitosan. Ruy-Shin Juang *et al*<sup>6</sup> reported similar observations while studying the adsorption of reactive dyes over chitosan.

### 3.7 Intraparticle diffusion

Sorption performances of chitosan are determined by the influence of diffusion mechanisms on zinc (II) uptake. Weber and Morris<sup>9</sup> pointed out that a functional relationship common to the majority of the intraparticle diffusion treatments is that the up-

take varies almost proportionately with the half power of time. The influence of intraparticle diffusion is estimated by evaluation of initial sorption rate. Figures 7 and 8 describe the plots of the sorption capacity,  $q_e$  against time squared. The  $k_p$  values given in tables 6 and 7 for the two different particle sizes are 3.04 and 0.75, and those for different doses are 3.04, 9.74 and 13.9 respectively. This shows that the initial slope of the curves indicating the sorption rate increases with doses and decreases with particle size of the material.<sup>16</sup>

### 3.8 Effect of temperature

The temperature dependence of zinc (II) by chitosan was studied over the range of 293–323 K. The considerable increase in the amounts of zinc (II) adsorbed with temperature confirms the endothermic nature of the process. The enhancement of adsorption capacity of chitosan, with temperature is attributed to the possible increase in the number of active sites available for adsorption on the surface.<sup>17</sup>

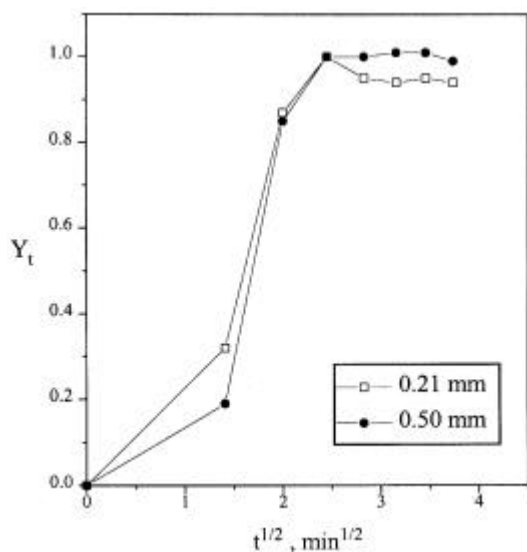


**Figure 5.** Time-dependence of the fraction of adsorption at different particle sizes of chitosan.

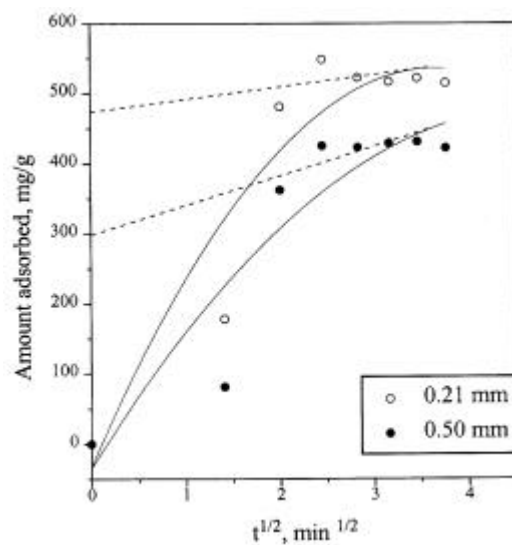


**Figure 7.** Intraparticle diffusion plot for the adsorption of zinc on chitosan at different particle sizes.

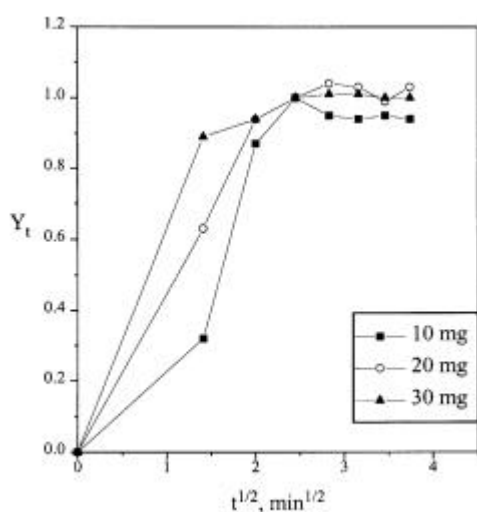


**Figure 6.** Time-dependence of the fraction of adsorption at different amounts of chitosan.

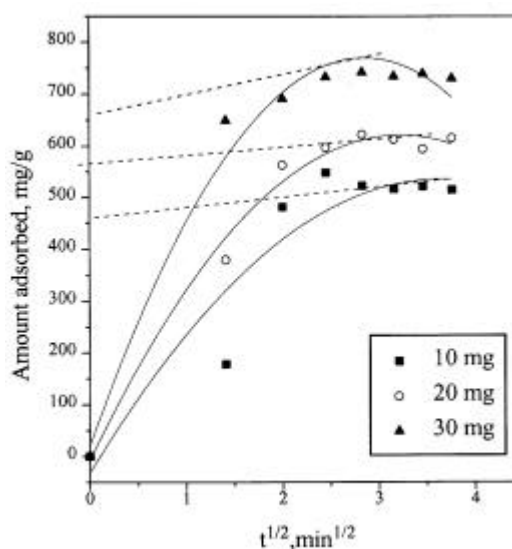


**Figure 8.** Intraparticle diffusion plot for the adsorption of zinc on chitosan at different dosages.

**Table 6.** Intraparticle diffusion rate constant.

Particle size (mm)	$k_p$ value
0.21	3.04
0.50	0.75

**Table 7.**

Dosage (mg)	$k_p$ value
10	3.04
20	9.74
30	13.90

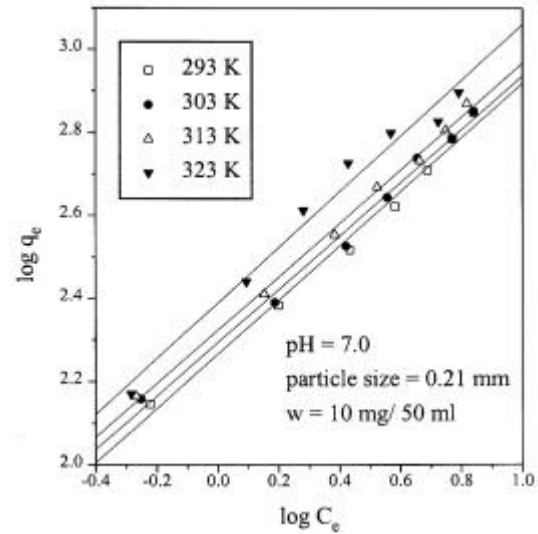
### 3.9 Effect of co-ions

The study of the influence of co-ions on the removal of zinc (II) ions becomes relevant when the selective adsorption of the metal ion occurs from the aqueous system. The experimental results revealed that the presence of foreign ions such as Fe (III), Cu (II) and Cr (VI) diminished the adsorption of zinc (II) ions. Maximum inhibition rate was caused by Cu (II) ions. This is attributed to the fact that the hydrated copper ions have smaller radii (0.419 nm) than hydrated zinc ions (0.430 nm) and thus have greater access to the surface of the adsorbent.<sup>18</sup> Jha *et al*<sup>13</sup> have also reported a similar co-ionic effect in the removal of specific metal ions in their studies using chitosan.

### 3.10 Adsorption isotherms

Freundlich<sup>19</sup> and Langmuir<sup>20</sup> adsorption isotherm models were applied to the system, studied at four temperatures.

**3.10a Freundlich isotherm:** Batch adsorption isothermal data, fitted into the linear form of the Freundlich isotherm is shown in figure 9 ( $\log q_e$  versus  $\log C_e$ ). The adsorption capacity,  $K$  and the adsorption intensity,  $1/n$  are directly obtained from the slopes and the intercepts of the linear plot, respectively and the data are provided in table 8. The  $K$ , which is a measure of adsorption capacity, increased with temperature. The magnitude of the exponent,  $n$  gives an indication of the favourability and capacity of the adsorbent/adsorbate system. Treybal<sup>21</sup> has reported that ' $n$ ' values between 1 and 10 represent favourable adsorption conditions.<sup>22</sup> In all cases re-

**Figure 9.** Freundlich isotherm.**Table 8.** Freundlich parameters.

Temperature (K)	$K$	$1/n$
293	2.2658	0.6529
303	2.2937	0.6422
313	2.3236	0.6428
323	2.3893	0.6707

ported here, the exponent is  $1 < n < 2$  showing beneficial adsorption for the system. The plot of  $\log q_e$  versus  $\log C_e$  for various initial concentrations is linear indicating the applicability of Freundlich adsorption isotherm ( $0.9894 < r < 0.9982$  and  $0.0163 < sd < 0.0408$ ). The fit of the data to the Freundlich model indicate that the forces of adsorption by chitosan are governed by physisorption.

**3.10b Langmuir isotherm:** Zinc(II)–chitosan system obeys the Langmuir adsorption isotherm. The  $C_e$  and  $C_e/q_e$  values and the Langmuir constants,  $Q$  and  $b$  for different temperatures calculated are presented in tables 9 and 10 respectively. The linear plots of  $C_e/q_e$  versus  $C_e$  ( $0.8977 < r < 0.9845$  and  $0.3298 < sd < 1.0437$ ) at the four temperatures indicate the applicability of Langmuir adsorption isotherm on the adsorption process occurring through a monolayer coverage. The Langmuir plots showing the increase in the rate of adsorption at higher temperatures are presented in figure 10. The  $C_e$  values of adsorbate in solution are higher at lower temperatures and they decrease with increasing temperature indicating greater adsorption at higher temperatures. The increasing trends observed in  $Q$  and  $b$  provided

**Table 9.** Effect of temperature on equilibrium parameters.

Concentration of zinc ion (mg/L)	$C_e$ (mg/L)				$C_e/q_e$ (mg/L)			
	Temperature (K)				Temperature (K)			
	293	303	313	323	293	303	313	323
2	0.60	0.56	0.54	0.52	3.19	3.89	3.70	3.51
4	1.58	1.54	1.42	1.24	6.53	6.26	5.50	4.49
6	2.71	2.64	2.42	1.91	8.24	7.86	6.76	4.66
8	3.82	3.60	3.34	2.68	9.14	8.18	7.17	5.04
10	4.89	4.52	4.60	3.70	9.57	8.24	8.52	5.87
12	5.91	5.88	5.60	5.30	9.70	9.61	8.75	7.91
14	6.93	6.90	6.58	6.19	9.80	9.71	8.86	7.93

**Table 10.** Langmuir constants and thermodynamic parameters.

Temp. (K)	Langmuir constants		Thermodynamic parameters			
	$b$ (L mg <sup>-1</sup> )	$Q$ (mg g <sup>-1</sup> )	$K_o$	$\Delta G^\circ$ (kJ mol <sup>-1</sup> )	$\Delta H^\circ$ (kJ mol <sup>-1</sup> )	$\Delta S^\circ$ (J mol <sup>-1</sup> K <sup>-1</sup> )
293	0.1703	1.1857	5.39	-4.09	2.2090	21.50
303	0.1778	1.2095	5.51	-4.30		
313	0.1985	1.2145	5.65	-4.52		
323	0.2546	1.2442	5.84	-4.73		

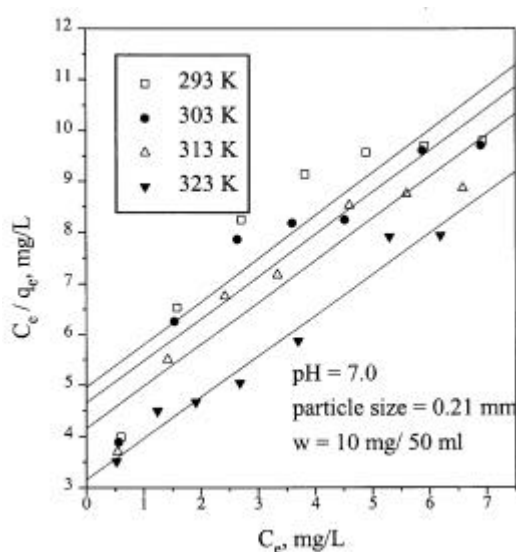


**Figure 10.** Langmuir isotherm.

in the table confirm the enhanced adsorption at higher temperature. The enhanced sorptive nature of chitosan at higher temperature is due to the swelling in the internal pores of the adsorbent to trap in more zinc ions on its surface. The above results are in good agreement with the earlier reports from this laboratory, pertaining to fluoride adsorption studies by dolomite.<sup>23</sup>

### 3.11 Equilibrium parameter

The essential characteristics of Langmuir equation can be expressed in terms of a dimensionless separation factor or equilibrium parameter,  $R_L$ .<sup>24</sup> These values indicate the shape of the isotherm to be either unfavourable ( $R_L > 1$ ), linear ( $R_L = 1$ ), favourable ( $0 < R_L < 1$ ) or irreversible ( $R_L = 0$ ). The values of  $R_L$  obtained for the zinc (II) – chitosan system are provided in table 11. The  $R_L$  values, for 2–14 mg/L of zinc ions in the solution, lying between 0 and 1, indicate favourable adsorption at four temperatures.

### 3.12 Adsorption dynamics

The thermodynamic equilibrium constants,  $K_o$  for the sorption reactions are determined by the method suggested by Khan and Singh<sup>25</sup> by plotting  $\ln(q_e/C_e)$  versus  $q_e$  (figure 11) and extrapolating to zero. The endothermic nature of adsorption is indicated by an increase in the  $K_o$  values with a rise in temperature. Thermodynamic parameters are calculated from the variation of the thermodynamic equilibrium constants  $K_o$  and the values are given in table 10. A plot of  $\ln K_o$  versus  $1/T$  is linear as indicated in figure 12.  $\Delta H^\circ$  and  $\Delta S^\circ$  are determined from the slopes and intercepts of the plot and the values are given in table

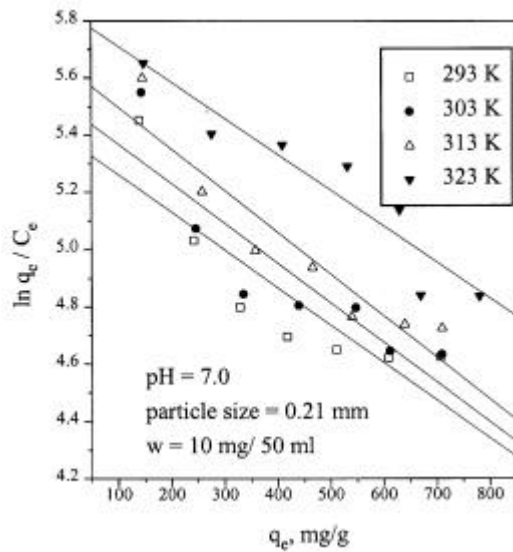


Figure 11. Plot of  $\ln q_e/C_e$  versus  $q_e$ .

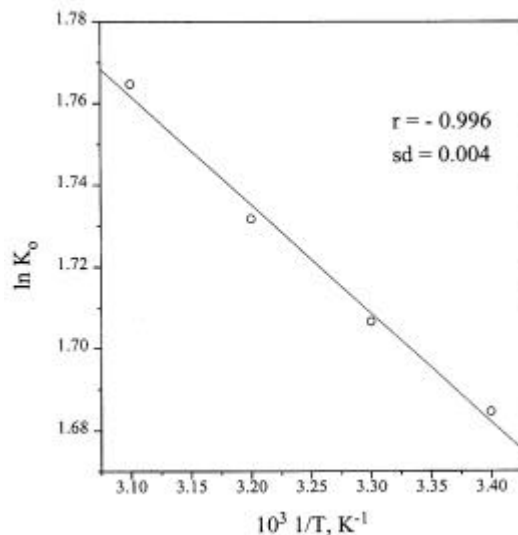


Figure 12. Plot of  $\ln K_0$  versus  $1/T$ .

10. The negative values of  $\Delta G^\circ$  indicate the feasibility of the process and also the spontaneity of adsorption reaction. The amount of zinc (II) adsorbed at equilibrium must increase with increasing temperature, because  $\Delta G^\circ$  decreases with the rise in temperature of the solution. This explains why the value of  $\Delta G^\circ$  is negative with the rise in temperature. The value of  $\Delta H^\circ$  (2.2090 kJ/mol) is positive and it confirms the endothermic character of the reaction. The positive value of  $\Delta S^\circ$  (21.50 J/K/mol) shows the increased randomness at the solid-solution interface during the adsorption of Zn (II) on chitosan.<sup>26</sup>

Table 11. Equilibrium parameter.

Concentration of zinc ion (mg/L)	Temperature (K)			
	293	303	313	323
2	0.746	0.738	0.716	0.663
4	0.595	0.584	0.557	0.495
6	0.495	0.484	0.456	0.396
8	0.423	0.413	0.386	0.329
10	0.370	0.360	0.335	0.282
12	0.329	0.319	0.296	0.247
14	0.295	0.286	0.265	0.219

#### 4. Conclusion

It is observed from the present study that an optimum contact period of six minutes is required for the maximum removal of zinc (II) by chitosan. The adsorption mechanism also depends upon the particle size of the adsorbent, pH of the medium and the presence of other anions like chlorides and nitrates. Also, the co-ions like Fe (III), Cu (II) and Cr (VI) were observed to inhibit the adsorption rate significantly. The fraction of adsorption increases with decrease in particle size and increase in the dosage of chitosan. The intraparticle diffusion rate constant,  $k_p$  is found to be maximum for smaller particle size and higher dose of the adsorbent. The adsorption mechanism obeys Freundlich and Langmuir equations indicating beneficial adsorption occurring through a monolayer mechanism involving physisorption and/or chemisorption. Thermodynamic and equilibrium parameters show that the adsorption process is endothermic and spontaneous, which implies increased sorption at higher temperatures.

#### References

1. Cunningham WP 1999 *Environmental encyclopedia* 2nd edn (Chennai: Jaia)
2. McKay G, Blair H S and Findon A 1989 *Indian J. Chem.* **A28** 356
3. Yang T C and Zall R R 1984 *Indian Eng. Chem. Prod. Res. Dev.* **23** 168
4. Ravi Kumar M N V 1999 *Bull. Mater. Sci.* **22** 905
5. Randall JM, Randall V G, McDonald GM and Young RN 1979 *J. Appl. Polym. Sci.* **23** 727
6. Ruey-Shin Juang, Ru-Ling Tseng, Feng-Chin Wu and Shwu-Hwa Lee 1997 *J. Chem. Technol. Biotechnol.* **70** 391
7. Guibal E, Jansson-Charrier M, Saucedo I and Le Cloirec P 1995 *Langmuir* **11** 591
8. Schmuhl R, Krieg H M and Keizer K 2001 *Water SA* **27** 1

9. Weber W J and Morris J C 1963 *J. Sanit. Engg. Div. ASCE* **89** (SA2) 31
10. Selvaraj K, Chandramohan V and Patabhi S 1998 *Indian J. Environ. Protect.* **18** 641
11. Parekh D C, Patel J B, Sudhakar P and Koshy V J 2002 *Indian J. Chem. Technol.* **9** 540
12. Gonzalez M, Magdalena Santana-Casiano J D and Millero F J 1990 *J. Colloid Interface Sci.* **137** 102
13. Jha I N, Leela Iyengar and Prabhakara Rao A V S 1988 *J. Environ. Engg.* **114** 962
14. Anirudhan T S and Sreedhar M K 1988 *Poll. Res.* **17** 381
15. Peniche-Covas C, Alvarez L W and Arguelles-Monal W 1992 *J. Appl. Polym. Sci.* **46** 1147
16. Raji C and Anirudhan T S 1998 *Ecol. Environ. Conserv.* **4** 33
17. Anoop Krishnan K and Anirudhan T S 2002 *Indian J. Chem. Technol.* **9** 32
18. Nightingale K R 1959 *J. Phys. Chem.* **63** 1381
19. Freundlich H 1926 *Colloid capillary chemistry* (London: Methuen)
20. Langmuir I J 1918 *J. Am. Chem. Soc.* **40** 1361
21. Treybal R E 1980 *Mass transfer operations* (New York: McGraw Hill)
22. Stephan Inbaraj B and Sulochana N 2002 *Indian J. Chem. Technol.* **9** 201
23. Karthikeyan G, Pius A and Alagumuthu G 2002 *Indian J. Chem. Technol.* **9** 397
24. Singh D K and Srivastava B 2001 *Indian J. Chem. Technol.* **8** 133
25. Khan A A and Singh R P 1987 *Colloid Surf.* **24** 33
26. Thomas R and Anirudhan T S 1999 *Indian J. Chem. Technol.* **6** 268